



HAL
open science

Analysis of thermoelastic and dissipative effects related to the fatigue of 2024 T3 aluminium alloy

Anna Eva Morabito, André Chrysochoos, Vito Dattoma, Umberto Galietti

► To cite this version:

Anna Eva Morabito, André Chrysochoos, Vito Dattoma, Umberto Galietti. Analysis of thermoelastic and dissipative effects related to the fatigue of 2024 T3 aluminium alloy. Quantitative InfraRed Thermography Journal, 2004, 1 (1), pp.99-116. 10.3166/qirt.1.99-116 . hal-03350390

HAL Id: hal-03350390

<https://hal.science/hal-03350390>

Submitted on 21 Sep 2021

HAL is a multi-disciplinary open access archive for the deposit and dissemination of scientific research documents, whether they are published or not. The documents may come from teaching and research institutions in France or abroad, or from public or private research centers.

L'archive ouverte pluridisciplinaire **HAL**, est destinée au dépôt et à la diffusion de documents scientifiques de niveau recherche, publiés ou non, émanant des établissements d'enseignement et de recherche français ou étrangers, des laboratoires publics ou privés.

Analysis of thermoelastic and dissipative effects related to the fatigue of 2024 T3 aluminium alloy

Anna Eva Morabito* — **André Chrysochoos**** — **Vito Dattoma***
— **Umberto Galietti*****

* *Department of Ingegneria dell'Innovazione – University of Lecce (Italy)*
annaeva.dattoma@unile.it
vito.dattoma@unile.it

** *Lab. de Mécanique et Génie Civil – Université Montpellier II (France)*
chryso@lmgc.univ-montp2.fr

*** *Department of Ingegneria Meccanica e Gestionale – Polytechnic of Bari*
galietti@poliba.it

ABSTRACT: In this paper the fatigue phenomena of 2024 T3 aluminium alloy were studied in terms of thermal and calorimetric effects during uniaxial cyclic loading. Thermoelastic coupling sources and dissipation were separately estimated by using infrared thermal data and a local simplified form of the heat equation. The simplifications are essentially based on the assumption that the uniaxial fatigue test remains homogeneous until a macroscopic fatigue crack occurs within the gauge section of the specimen. Heat sources were then compared to predictions derived from mechanical data by assuming a linear isotropic thermoelastic behaviour of the material and by neglecting the influence of thermomechanical couplings on the hysteresis area of fatigue cycles.

KEYWORDS: aluminium, fatigue, infrared thermography, thermomechanical couplings, dissipation.

1. Introduction

The traditional methods used for characterizing the fatigue behaviour of materials require series of cyclic loading tests which are time-consuming and expensive. In particular, methods such as *staircase* method or *Probit* method, or those consisting in plotting the Wöhler curves imply long and repetitive tests to get the fatigue limit.

The development of electrodynamic resonance machines has permitted to increase consistently the frequency of cyclic loading and then to speed up the fatigue tests. However, these techniques must be used with attention especially when the material behaviour is sensitive to strain-rate or temperature changes.

The fatigue behaviour analysis is even more delicate for aluminium alloys because the Wöhler curves of aluminium do not show any asymptotic stress classically associated with the fatigue limit (Bathias *et al.*, 1997).

It is so explained why there is an increasing interest in alternative experimental approaches which may provide more rapidly reliable fatigue characteristics.

Among these, the methods based on the analysis of the self-heating during a stepwise loading fatigue test must be mentioned. The remarkable change of the heating regime at a certain stress range was empirically related to the fatigue limit of material (Luong 1998, La Rosa *et al.* 2000). These methods already provided reliable fatigue limit values for some steels (Morabito *et al.*, 2002). However, the results are more questionable for aluminium alloys, mainly because of the high thermal diffusivity of these materials (Krapez *et al.*, 2000).

The thermal increase can be considered as an indicator of fatigue irreversibility, but its practical use can be problematic since it does not reveal the intrinsic behaviour of material. In fact it depends on the diffusion properties (material effect) but also on thermal boundary conditions and on intensity and distribution of heat sources (structure effect). For these reasons an estimation of the different heat sources was chosen as representative of the fatigue phenomena. The aim of this work is to construct energy balances to get progressively a better understanding of the fatigue phenomena in relation with the microstructure mechanisms.

In this paper the fatigue phenomena of 2024 T3 aluminium alloy were studied in terms of thermal and calorimetric effects during uniaxial cyclic loading test. The paper is composed as follows: after a brief recall of the thermodynamic framework used to construct the local heat equation and to define the different heat sources, the infrared image processing techniques developed to estimate separately the heat source due to thermoelasticity and the energy dissipation is detailed. The local simplified heat equation is based on the assumption that the conditions of the uniaxial fatigue test, that is material mechanical and thermal properties, remain homogeneous until a macroscopic fatigue crack occurs within the gauge section of the specimen. Heat source estimates are then compared to predictions derived from mechanical data by assuming a linear isotropic thermoelastic behaviour and by neglecting the influence of thermomechanical couplings on the hysteresis area of fatigue cycles.

2. Thermodynamic Framework

The thermomechanical framework used to interpret the experimental results is the Thermodynamics of Irreversible Processes that is based on the local state axiom and consequently characterizes the equilibrium state of each volume material element by a set of N state variables. The selected variables are: the absolute temperature T , the strain tensor under the small perturbation hypothesis ε and $N-2$ internal variables α_i describing, at macroscopic level, complex and often coupled microstructural phenomena. Using the formalism of Generalized Standard Materials it is possible to sum-up the material behaviour by means of a thermodynamic potential and a dissipation potential. By construction, the thermodynamic potential is the specific Helmholtz free energy $\Psi(T, \varepsilon, \alpha_i)$ and the potential dissipation is a function of the flux of state variables, that is $\varphi(\bar{q}, \dot{\varepsilon}, \dot{\alpha}_i; T)$, \bar{q} being the heat influx and T acting as a parameter (Germain 1973, Lemaitre *et al.* 1990).

The derivatives of Ψ with respect to the state variables give the following state equations:

$$\begin{cases} s = -\Psi_{,T} \\ \sigma^r = \rho \Psi_{,\varepsilon} \\ A_i = \rho \Psi_{,\alpha_i} \end{cases} \quad [1]$$

where s is the specific entropy, σ^r the reversible stress tensor, and A_α/ρ the conjugated variable associated with α . To describe the dissipation mechanisms and consequently the evolution of internal variables, complementary equations are needed. They are expressed from the derivatives of φ with respect to the flux variables:

$$\begin{cases} \sigma^{ir} = \varphi_{,\dot{\varepsilon}} \\ -A_i = \varphi_{,\dot{\alpha}_i} \\ -\text{grad}T/T = \varphi_{,q} \end{cases} \quad [2]$$

where σ^{ir} is the irreversible stress tensor and $-A$ is the thermodynamic force associated with α . Combining first and second principles of thermodynamics leads to the local heat equation:

$$\rho C \dot{T} - \text{div}(K : \overline{\text{grad}T}) = d_1 + T \sigma_{,T}^r : \dot{\varepsilon} + T A_{i,T} \dot{\alpha}_i + r_{\text{ext}} \quad [3]$$

where ρ , C and K stand respectively for the mass density, the specific heat, the conduction tensor.

The left-hand member of equation (3) is a differential operator applied to T while the right hand member groups all the possible heat sources accompanying the deformation process. We find in turn: the intrinsic dissipation $d_1 = \sigma^{ir} : \dot{\epsilon} - A_i \dot{\alpha}_i$, the thermoelastic source $s_{the} = T \sigma_{,T}^r : \dot{\epsilon}$, the “internal” coupling sources $s_{ic} = T A_{i,T} \cdot \dot{\alpha}_i$ and the external volume heat supply r_{ext} .

The overall heat source can then be estimated by evaluating the left hand side of heat equation thanks to the thermal fields given by the infrared camera (Chrysochoos *et al.* 1995).

The fatigue processes can be considered as quasi-static under the small perturbations hypothesis. Besides, the following hypotheses are formulated:

- the heat conduction is isotropic and the related coefficient k remains constant during the test;
- the density ρ and the specific heat C are material constants, independent from the internal state;
- the convective terms, included in the material time derivation are neglected;
- the external heat supply r_{ext} (in this case only due to radiation heat exchanges) is time-independent. Consequently the equilibrium temperature field T_0 verifies the following equation:

$$-k \Delta T_0 = r_{ext} \quad [4]$$

- the temperature variations $\theta = T - T_0$ induced by fatigue mechanisms are too small to have any influence on the micro-structural state. Consequently it is possible to state $s_{ic} = 0$.

Under these hypotheses it is possible to write the local heat equation in the following compact and simplified form:

$$\rho C \frac{\partial \theta(x, y, z, t)}{\partial t} - k \Delta \theta(x, y, z, t) = s(x, y, z, t) \quad [5]$$

where $s = d_1 + s_{the}$ is the overall volume heat source.

3. Data Processing

The final aim of the data processing is to evaluate the heat sources throughout the specimen gauge part by using discrete and noisy surface temperature measurements. This problem, in the general tri-dimensional (3D) case, is impossible

to solve without any information about heat source distribution (Capatina *et al.* 2000). However, if thermal gradients remain small throughout the thickness, an averaged heat sources distribution can be estimated, by integrating Eq. (5) throughout the thickness, assuming that the measured surface thermal map is very close to the depth-wise averaged temperature field $\bar{\theta}(x, y, t)$. This approach was successfully used to track localization zones during monotonic tensile tests (Chrysochoos *et al.* 2000).

In the case of fatigue of aluminium alloys this bi-dimensional (2D) approach is still strongly unstable from a numerical point of view because of the low signal-to-noise ratio. The next possibility is then to consider a one-dimensional (1D) diffusion problem which leads to an estimate of the mean heat source over each sample cross section S. The integration of Eq. (5) leads to:

$$\rho C \left(\frac{\partial \bar{\theta}(x, t)}{\partial t} + \frac{\bar{\theta}(x, t)}{\tau_{th}^{1D}} \right) - k \frac{\partial^2 \bar{\theta}(x, t)}{\partial x^2} = \bar{s}(x, t) \quad [6]$$

where the mean temperature of the cross-section $\bar{\theta}$ is identified with the surface temperature. The time constant τ_{th}^{1D} characterizes the lateral heat exchanges by conduction, convection and radiation between the specimen and the surroundings. These exchanges are supposed to be proportional to the temperature variation.

In order to estimate the left-hand member of Eq. (6), longitudinal temperature profiles were built by averaging the surface temperature over the specimen width.

However under the hypothesis that the mechanical test is homogeneous, the heat equation can be further simplified. Indeed, an analysis of the spectral solution of the heat equation leads to write in such a case (Chrysochoos 1995):

$$\rho C \left(\frac{d\theta_c(t)}{dt} + \frac{\theta_c(t)}{\tau_{eq}} \right) \approx s = s_{the} + d_1 \quad [7]$$

where θ_c is now the temperature measured in the central part of the specimen. The time constant τ_{eq} characterizes all the local heat losses and can be evaluated by exponential regression of thermal equilibrium return curves obtained after a homogeneous heating. Eq. (7) represents a local (0D) heat diffusion equation. We underline that the homogeneity hypothesis is perfectly consistent with the classical view of uniaxial tests.

The linearity of Eqs.(6-7) and those of boundary conditions permits to study separately the influence of dissipative and thermoelastic sources on the temperature variation. Lets define θ_{the} and θ_d the thermoelastic and dissipative components of the temperature signal during a fatigue tensile test.

If no irreversibility is associated with the strain-rate (i.e. $\dot{\sigma}^{ir} = 0$), the thermoelastic volume source is defined by the following equation:

$$s_{\text{the}} = T \sigma_{,T} : \dot{\epsilon} \quad [8]$$

Besides, if the thermoelastic behaviour is homogeneous, linear and isotropic then it is possible to get :

$$s_{\text{the}} \approx -\alpha T_0 \dot{\sigma} \quad [9]$$

where σ denotes the uniaxial stress, E the Young's modulus and α the linear thermal expansion coefficient. In Eq.(9), the approximation is valid for tests close to thermal equilibrium ($\theta \ll T_0$) and as far as $E\alpha^2 T_0 / \rho C \ll 1$.

For a sinusoidal loading $\sigma(t) = \sigma_m + \frac{\Delta\sigma}{2} \sin(2\pi f_L t)$ defined by a mean stress σ_m , a stress range $\Delta\sigma$ and a loading frequency f_L , it is easy to verify that :

- the temperature variation has the same frequency spectrum as the stress signal;
- the thermoelastic energy vanishes at the end of each loading cycle.

The range of the thermoelastic source can also be determined:

$$\Delta s_{\text{the}} = 2\pi f_L \alpha T_0 \Delta\sigma \quad [10]$$

Moreover, when solving the differential equation

$$\frac{d\theta_{\text{the}}}{dt} + \frac{\theta_{\text{the}}}{\tau_{\text{eq}}} = -\frac{\alpha T_0}{\rho C} \dot{\sigma} \quad [11]$$

the thermoelastic temperature range takes the following form:

$$\Delta\theta_{\text{the}} = \frac{T_0 \alpha \Delta\sigma}{\rho C} \frac{2\pi f_L}{\sqrt{\tau_{\text{eq}}^{-2} + 4\pi^2 f_L^2}} \quad [12]$$

Note that the thermal thermoelastic range becomes f_L -independent for frequencies such that $f_L \gg f_L^0 = \frac{1}{2\pi\tau_{\text{eq}}}$.

The assessment of heat source distribution, by means of Eq.(6) or Eq.(7), requires the evaluation of partial differential operators. Derivation of noisy digital signal decreases the signal-to-noise ratio. It is consequently important to reduce the noise amplitude without modifying the thermal gradients.

Among the several possible methods, in this work a local least squares approximation of the thermal signal with an appropriately selected function set is used (Boulanger *et al.* 2004). For example, in the case of 0D diffusion problem, the local temperature can be approximated by:

$$\theta(t)=at+b+c\sin(2\pi f_L t+d) \quad [13]$$

The linear terms describe a slowly varying dissipative effect and possible transient thermal effects, while the trigonometric function is related to the periodic thermoelastic effects.

Another way can be followed to reach mean values of the dissipated energy. This way is based on stress and strain measurements. Let us call A and B two thermodynamic states defining a mechanical cycle of the fatigue test. The hysteresis area A_h of the loop is by construction:

$$A_h = \int_{t_A}^{t_B} \sigma : \dot{\varepsilon} dt \quad [14]$$

If the hysteresis loop is also a thermodynamic cycle, it is possible to show that (Peyroux *et al.* 1998):

$$A_h = \int_{t_A}^{t_B} d_1 dt + \int_{t_A}^{t_B} \theta \sigma_{,T} : \dot{\varepsilon} dt + \int_{t_A}^{t_B} \theta A_{,c_i} \dot{c}_i dt \quad [15]$$

In the case under examination, contribution due to the “internal” coupling sources are negligible and the thermoelastic source vanishes at the end of each cycle so that the hysteresis area measurement gives an estimate of the mean dissipation during a cycle of the fatigue test:

$$A_h \approx \int_{t_A}^{t_B} d_1 dt \quad [16]$$

For homogeneous mechanical tests (0D approach), the mean dissipation per cycle is then proportional to the hysteresis area of the load-displacement loop.

4. Experimental Tools

The material under investigation is 2024 T3 aluminum alloy in which the major alloying element is copper. The T3 temper indicates the thermo-mechanical treatment including solution heating, cold working and naturally ageing. Thermophysical properties are given in Table 1.

The Table 2 presents some basic mechanical properties derived from experimental tests at room temperature.

Table 1. *Thermophysical properties of 2024 T3 aluminum alloy*

ρ [Kg/m ³]	C [J/KgK]	k [W/mK]	α [1/K]
2770	875	120	$2.11 \cdot 10^{-5}$

Table 2. *Room temperature mechanical properties of 2024 T3 aluminum alloy*

E [MPa]	R _{p0.2} [MPa]	R _{p0.02} [MPa]	Tensile strenght [MPa]	Fatigue strenght (R _σ =0.1) [MPa]
72000	350	310	480	120

Concerning the fatigue behaviour, the difficulties encountered to define a conventional fatigue limit with Wöhler curves have been already mentioned. For this reason the axial fatigue strenght at 10^7 cycles will be considered as reference value. This value (expressed in Table 2 in terms of stress range) is derived from axial classical fatigue tests at 30 Hz and with load ratio $R_\sigma = 0.1$.

The fatigue tests presented hereafter are carried out by imposing a series of loading blocks which start from stress levels lower than the fatigue reference value above-mentioned. Each block is performed at constant loading frequency f_L , constant load ratio R_σ , and constant stress range $\Delta\sigma$.

The tests are conducted by means of MTS servo-hydraulic machine equipped with ± 25 kN load cell. Flat specimens are used with gauge part volume equal to $3 \times 15 \times 10$ mm³. The experimental set-up includes a FPA infrared camera (Cedip SW). The maximum frame-rate of the IR camera is 250 images per second, each image being made of 64×120 pixels. During the tests the infrared device is placed in

front of the specimen, the lens axis being fixed and perpendicular to specimen surface. The space resolution is approximately equal to 0.2 mm/pixel.

The measurements of hysteresis area are performed by using a classical extensometer whose the gauge length is equal to 10 mm; we chose the ± 0.15 mm displacement range to get more accurate measurements. Note that the clamping system of the extensometer (rubber bracelets) allows us load frequencies up to 1 Hz.

5. Experimental results

Figure 1 shows the evolution of the temperature variation θ_c during the progression of the loading blocks (0D analysis). Each block is made of 20000 cycles performed at $f_L=50$ Hz. The temperature signal is sampled at $f_S=19$ Hz. The drift accompanying the oscillatory thermoelastic response comes from the transient effect associated with the progressive equilibrium of the heat losses, from the intrinsic dissipation, and from the always possible variation of the room temperature. At the end of each loading block, the thermal equilibrium is awaited before the next block starts. The corresponding thermal return has not been plotted in Figure 1.

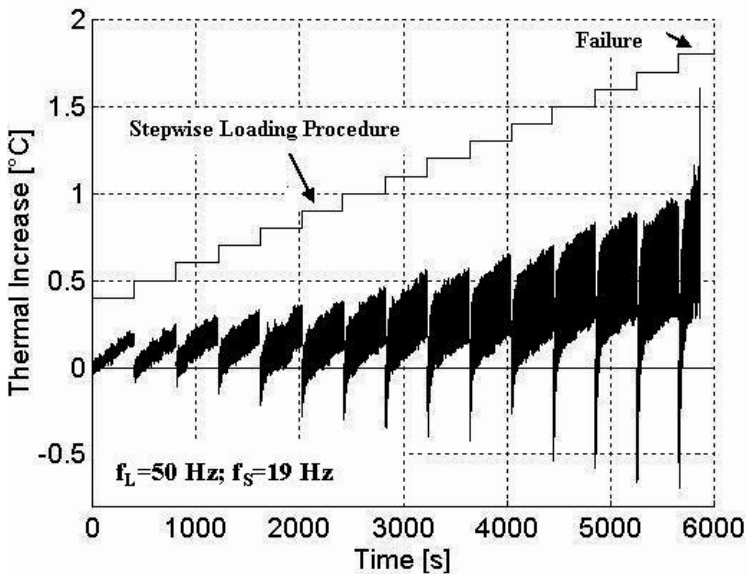


Figure 1. θ_c variations during a series of loading blocks

5.1 Analysis of thermoelastic sources

By using a local least squares method (see Eq.(13)), it is possible to separate the oscillatory component from the thermal drift.

The reliability of this operation naturally depends on the quality of the loading signal that has to be as monochromatic as possible. The periodic part of the thermoelastic temperature θ_{the} has been plotted in Figure 2.

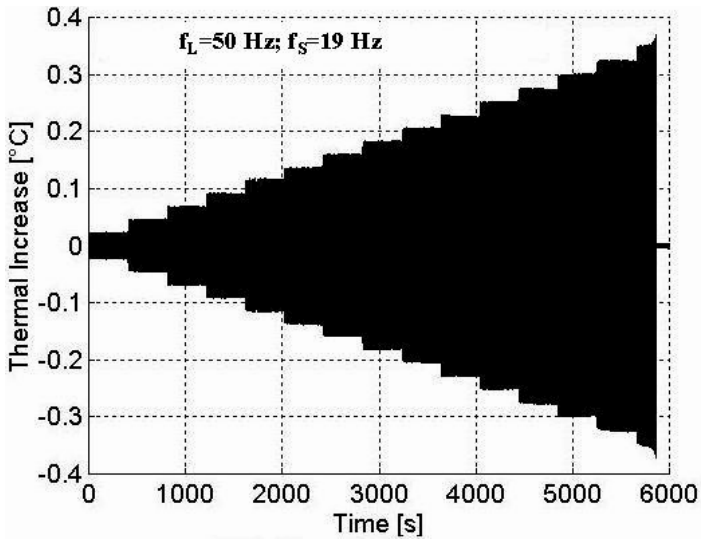


Figure 2. Periodic part of θ_{the}

The invariability of the stress range during a block is consistent with the evolution of $\Delta\theta_{the}$ (Eq.(12)) defined by the envelope curves of the periodic part of θ_{the} .

In Figure 3, it is possible to check the rate-independence of $\Delta\theta_{the}$ as soon as $f_L \gg f_L^0 \approx 0.07 \text{ Hz}$.

The thermoelastic temperature ranges have been plotted for all loading blocks and for two loading frequencies ($f_L = 1 \text{ Hz}$, $f_L = 50 \text{ Hz}$).

By using Eq.(7), the thermoelastic source ranges have been derived. The evolution of $\Delta s_{the}/\rho C$ is plotted in Figure 4.

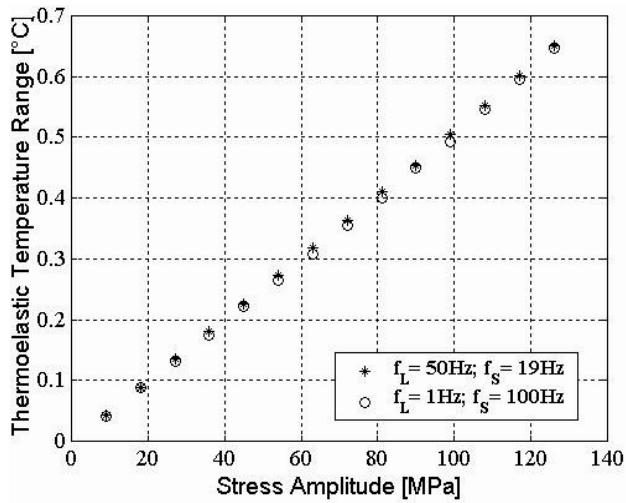


Figure 3. f_L -independence of $\Delta\theta_{the}$; (*: $f_L=50$ Hz; o: $f_L=1$ Hz)

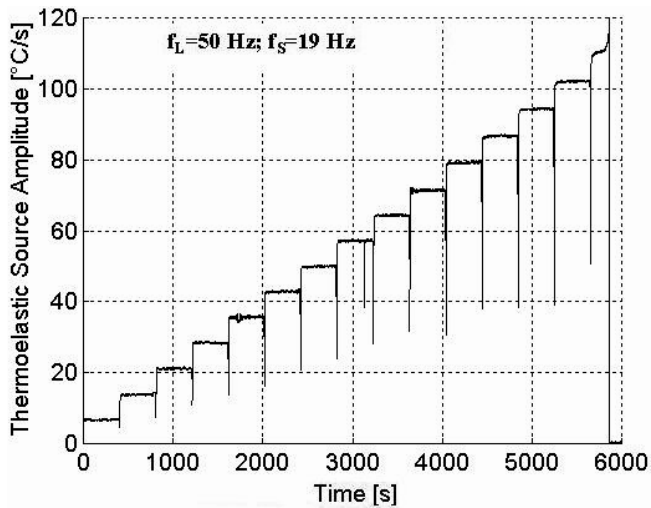


Figure 4. Thermoelastic source range $\Delta s_{the}/\rho C$ at $f_L=50$ Hz

It is convenient to “normalize” the heat source range values by dividing by ρC . This operation, in fact, gives an indication of magnitude of the warming (or cooling) speed if the processes were adiabatic. The new unit of this “normalized” heat source is indeed $^{\circ}\text{C}\cdot\text{s}^{-1}$.

Since the stress range is constant during each block, it is consistent to observe a stepwise constant evolution of thermoelastic source range. Nevertheless, as the stress range increases regularly, a constant progression of the thermoelastic plateau from one block to another should be seen, according to Eq.(10). In fact a slight deviation can be observed in Figure 4. To underline more precisely this deviation, a series of blocks has been performed at $f_L=1$ Hz in “over-sampling” conditions ($f_S=100$ Hz). The results are shown in Figure 5 where the solid line corresponds to the theoretical thermoelastic response. The slope of this straight line has been computed by considering the seven first blocks. The line spotted by squares groups the experimental data.

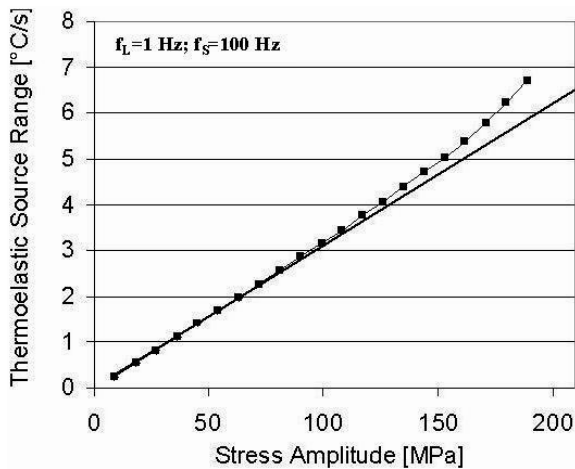


Figure 5. Progressive deviation of $\Delta s_{the}/\rho C$ at $f_L=1$ Hz

This deviation has already been observed in terms of temperature variations by some authors for other aluminium alloys (Krapez *et al.* 2000). These authors interpreted this effect in terms of non linear thermoelastic material behaviour, the Young’s modulus being supposed to be a function of the temperature.

5.2 Analysis of dissipation

The temperature drift is plotted in Figure 6. The noise is in this case due to the local fitting of the data. The negative values of the temperature observed at the beginning of each block can be related to the initial dissymmetry of the thermal response of a pure thermoelastic material during a load-unload cyclic test. Cycle by cycle, the heat losses make progressively the temperature variation periodic and symmetric.

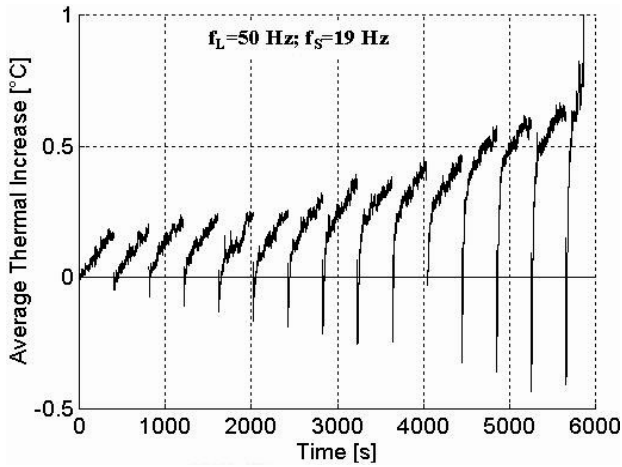


Figure 6. Thermal drift associated with Figure 1

The positive values of the drift can naturally be associated with the dissipation. However if it is supposed that the dissipative mechanisms accompanying the fatigue test change slowly, the dissipation should remain approximately constant during one block and the warming of the specimen should be limited by the heat losses. Indeed, many authors have observed this stationary state which is the main peculiarity of the thermal methods developed to assess rapidly the fatigue limit (Luong 1998, La Rosa *et al.* 2000). As it has been already said, these methods gave satisfactory results in the case of steels for which the stationary thermal drift may reach up to several tens of Celsius degrees.

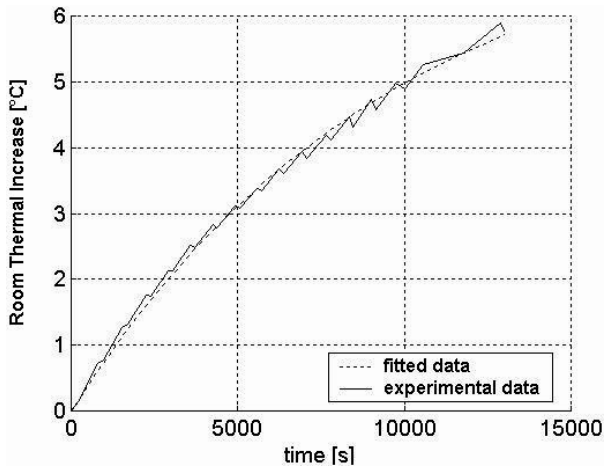


Figure 7. Evolution of T_0 during a fatigue test

This is not the case for the 2024 alloy for which the warming hardly exceeds 1°C at $f_L=50$ Hz. In such a situation it is necessary to check accurately the stability of the equilibrium temperature T_0 used in the thermal model to define the temperature variation q (Eq.(4)).

In Figure 7, the temperature evolution of the “equilibrium” temperature T_0 is presented. Compared to the self-heating of the specimen, these variations are not negligible (around 0.2 °C per block). Fully aware of this parasitic effect, θ_d has been nevertheless identified with the thermal drift.

In Figure 8 the trend of the dissipation (divided by ρC) obtained by the 0D thermal approach (Eq.(7)) is shown.

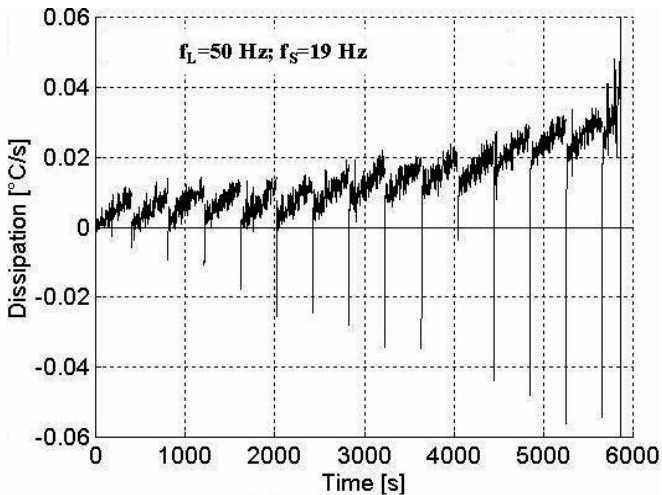


Figure 8. Estimates of $d/\rho C$ by using the 0D thermal model

This graph just gives an order of magnitude of the mean dissipation during a fatigue block. It is remarkable to underline that these dissipation amplitudes are at least 10^3 smaller than the ones of thermoelastic sources given in Figure 3.

To check these global dissipation estimates an extensometer to compute the hysteresis area of the cyclic load-displacement curves has been used (Eq.(16)).

In Figure 9, the mechanical estimates of the mean dissipation per cycle are plotted during a fatigue test performed at $f_L = 1$ Hz for a sampling frequency $f_S = 50$ Hz.

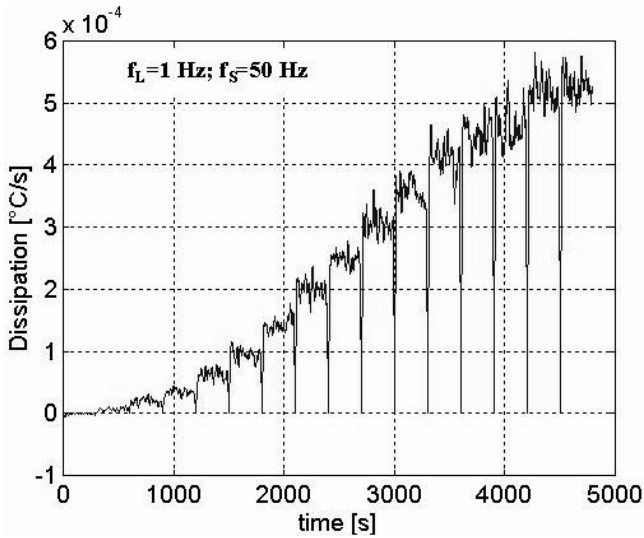


Figure 9. Estimates of $d_1/\rho C$ via hysteresis area measurements

Comparing mechanical and thermal estimates of dissipation is quite problematic for aluminium because the clamping system of the extensometer becomes unstable at high f_L , while, at low f_L , the thermal drift is essentially due to the warming of the testing machine. To short-cut this difficulty, the dissipation property has been studied by testing several small loading frequencies.

In Figure 10, the mean dissipation per cycle divided by the loading frequency are reported for two fatigue tests respectively performed at $f_L = 1$ Hz and $f_L = 0.5$ Hz (with $f_S = 25$ Hz).

This figure clearly shows that dissipation is proportional to f_L . From a thermodynamic point of view, this kind of result is interesting in order to qualify the irreversibility accompanying the fatigue test. The mechanical results obtained at low frequencies are in agreement with the dissipation model introduced in plasticity theory even if the stress level is, obviously, under the macroscopic yield stress.

If this dissipation property is now admitted for higher loading frequencies, it is possible to compare the mechanically predicted values of dissipation at $f_L = 50$ Hz with those thermally obtained.

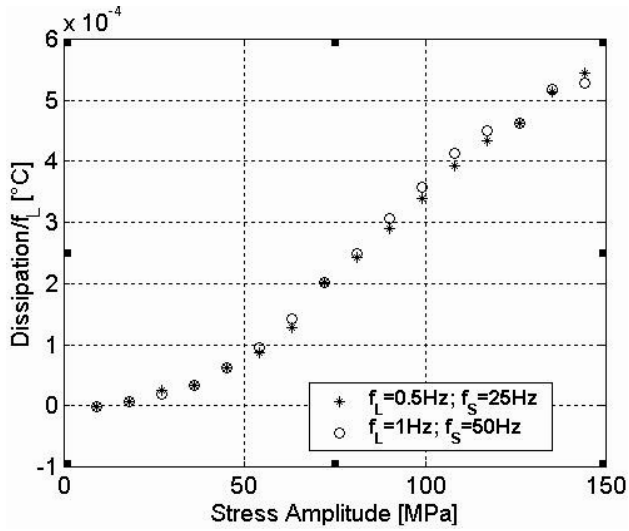


Figure 10. Estimates of $d_1/\rho C / f_L$ for two loading frequencies

Figure 11 shows this comparison. At low stress ranges, a scattering of the data is observed. Conversely for stress ranges greater than 60 MPa, the comparison is quite good. The divergence at low stress levels is not surprising if we remember that the thermal drift of the testing machine induces a bad signal-to-noise ratio.

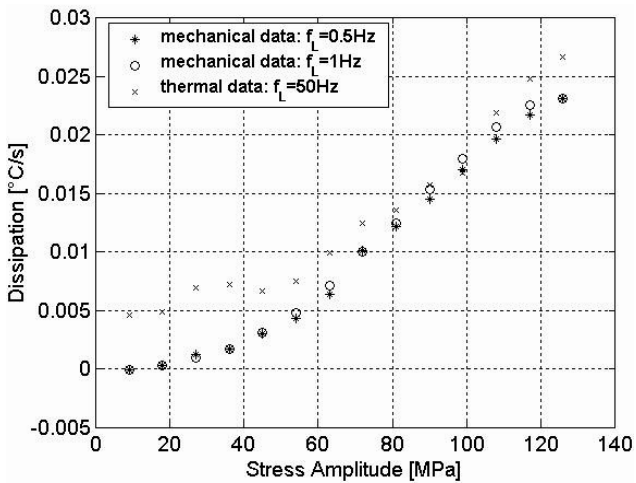


Figure 11. Comparison of thermal and mechanical estimates of $d_1/\rho C$

6. Conclusions

In this paper an energy analysis of the fatigue phenomena for an aluminium alloy is developed. By means of a convenient thermomechanical framework two energy pointers are identified: the thermoelastic source range and the energy dissipation.

The evaluation of these heat sources is based on the homogeneity hypothesis of the fatigue test. This hypothesis allowed to strongly simplify the thermal model used to compute the different heat sources.

This first attempt led to observe some limits of the macroscopic thermoelastic model: indeed, if the thermoelastic coupling source is well proportional to the loading frequency, a slight non linearity occurs when stress ranges tend toward the macroscopic yield stress. Some problems related to the dissipation evaluation are also identified. First, the dissipation amplitudes remain very small in comparison with the ranges of the thermoelastic source. Second, the aluminium alloy has a high diffusivity coefficient when compared to usual steels. Consequently, the thermal stability of the room temperature and of the testing machine becomes of fundamental importance for determining the real thermal drift related to the energy dissipation.

To short-cut temporarily this problem, the dissipation has been studied from a mechanical point of view. The first results are satisfactory: a linear evolution of the mean dissipation per cycle as a function of the loading frequency (for low fatigue frequencies) has been shown. Moreover, the extrapolated data at $f_L=50$ Hz are in good agreement with the dissipation estimates deduced from thermal data (for high stress ranges).

In order to check the validity of the homogeneity hypothesis of fatigue test, the thermal images processing procedure has to be improved in order to be able to construct at least 1D distribution of heat sources by using Eq.(6). In this way it will be possible to establish if, in the case of an aluminium alloy, the above-mentioned heat sources can be used in order to predict the potential onset zones of fatigue damage.

References

- Bathias C., Baïlon J. P., *La fatigue des matériaux et des structures*, Editions Hermès 1997
- Luong M. P., Fatigue limit evaluation of metals using an infrared thermographic technique, *Mechanics of Materials*, 28, 1998, p. 155-163.
- La Rosa G., Risitano A., Thermographic methodology for rapid determination of the fatigue limit of materials and mechanical components, *International Journal of Fatigue*, 22, 1, 2000, p. 65-73.
- Morabito A.E., Dattoma V., Galietti U., Energy -analysis of fatigue damage by thermographic technique, Proceedings, XXIV *Thermosense Conference*, 4710, p. 460-467, 2002.

- Krapez J.C, Pacou D., Gardette G., Lock-in thermography and fatigue limit of metals, *Proceedings, QIRT 2000*, 2000, p. 277-282.
- Germain, P., *Cours de mécanique des milieux continus*, 1, Masson Editeurs 1973.
- Lemaitre J., Chaboche J.L., *Mechanics of solid Materials*, Cambridge University Press, 1990.
- Chrysochoos A., Analyse du comportement des matériaux par thermographie infrarouge, *Proceedings, Photomécanique 1995*, p. 203-211.
- Capatina A., Stavre R., Algorithms and convergence results for an inverse problem in heat propagation, *International Journal of Engineering Science*, 38, 2000, p.575-587.
- Chrysochoos A., Louche H., An infrared image processing to analyse calorific effects accompanying strain localisation, *International Journal of Engineering Science*, 38, p. 1759-1788, 2000.
- Boulangier T., Chrysochoos A., Mabru C., Galtier A., Calorimetric analysis of dissipative and thermoelastic effects associated with the fatigue behaviour of steels, *International Journal of Fatigue*, 26, 2004,221-229.
- Peyroux R., Chrysochoos A., Licht C., Löbel M., Thermomechanical couplings and pseudoelasticity of shape memory alloys, *International Journal of Engineering Science*, 36, 1998, p. 489-509.